

In-Situ observation of isothermal CaSiO_3 crystallization in $\text{CaO-Al}_2\text{O}_3\text{-SiO}_2$
melts: a study of the effects of temperature and composition

Jing-Jing Liu^{1*}, Gong Chen¹, Peng-Cheng Yan¹, Bart Planpain¹, Nele Moelans¹ and Muxing
Guo¹

¹*Department of Metallurgy and Materials Engineering (MTM),*

KU Leuven, B-3001 Heverlee, Belgium

Abstract

The crystallization behavior of CaSiO_3 in different $\text{CaO-Al}_2\text{O}_3\text{-SiO}_2$ melts was comprehensively investigated in-situ with a confocal scanning laser microscope (CSLM) over a wide range of temperatures. The observations clearly indicate a transition from a faceted to dendritic crystal morphology with decreasing temperature. The undercooling required for dendritic growth increases with decreasing Al_2O_3 (under same basicity) and increasing basicity. The dendrite structure becomes finer at higher growth rates with a lower Al_2O_3 and higher basicity. The growth rates of different dendrites are time-independent. With increasing temperature, the growth rate first increases and then decreases. The observed dendrite tip radii are compared with those obtained from Ivantsov theory in 2D and 3D. With decreasing temperature, the growth conditions in the CSLM experiments appeared to shift from close to 3D (with the dendrite tip below the surface melt) to close to 2D (with the dendrite tip on top of the surface melt).

Keywords: A1. Dendrites, A1. Crystal morphology, A1. Diffusion, A1. Crystallites,
A2. Growth from high temperature solutions, B1. Oxides.

*Corresponding author: Jingjing Liu, email: jingjing.liu@mtm.kuleuven.be

Tel. +32-16-321245, Fax. +32-16-321991

1. Introduction

Triclinic Wollastonite with a space group of P-1 and a CaO/SiO₂ ratio of 1 (CaSiO₃) is an important ceramic raw material and a common additive in metallurgical applications. The combination of a low thermal conductivity, a moderate melting point (1540°C), high crystallization capacity and a low viscosity at high temperatures makes it a suitable candidate to serve as mould flux^{1, 2}. It can be used to prevent the meniscus of the molten steel from oxidation, insulate the molten steel to avoid freezing, provide liquid lubrication for the strand and control the heat transfer between the strand and mould during the continuous casting of steel². Furthermore, CaSiO₃ absorbs easily Al₂O₃ to form Anorthite or Gehlenite. As a result, Wollastonite has been widely used to remove Al₂O₃ based inclusions in liquid steel to meet the increasing demand for high cleanliness steel worldwide³.

In many applications of CaSiO₃ based mould fluxes, the crystallization behavior is of great importance. For instance, the morphology of CaSiO₃ particles has an impact on the thermal resistance at the interface between mold flux film and copper mould. Crystallization of such a slag influences the mineralogy of the cooled slag after tapping as well. Moreover, a deeper understanding of the crystallization behavior of the molten slag will be of significant importance to obtain glassy materials with superior mechanical properties through a controlled crystallization of a heavily undercooled liquid^{4, 5}. These important aspects drive us to take the crystallization of CaSiO₃ in a CaO–Al₂O₃–SiO₂ melt as the main research topic here.

A number of techniques have been developed to investigate the slag crystallization, including DTA (Differential Thermal Analysis) and Single (or Double) Hot Thermocouple Technique (SHTT or DHTT) ⁶. Both techniques have their limitations. For DTA, it is difficult to observe the crystallization process directly and also hard to realize rapid quenching, since the heating is done by an electric furnace having relatively large thermal inertia ⁷. The SHTT or DHTT technique can only obtain information on the sample surface at high temperature and the collected pictures always have a relatively low resolution.

An alternative way to observe the high temperature crystallization processes can be realized by a hot stage confocal laser microscope (CSLM)⁸, in which the utilization of a laser and the light detector (only the light reflected from the focal plane arrives at the detector) results in a high illumination intensity and a very sharp axial resolution between different phases. Furthermore, several isothermal observations can be done in a single experiment, which significantly improves the efficiency⁸⁻¹⁰. The CSLM technology has been successfully applied to observe the collision, agglomeration, and cluster formation of Al₂O₃ and CaO-Al₂O₃ inclusions on the surface of molten steel samples¹¹. A number of in-situ observations of the dissolution of refractory particles in slags using CSLM have also been reported⁸⁻¹⁰. However, very limited work has been done on the crystallization of oxide melts using CSLM. C. Orrling et al. investigated the crystallization behavior of CaO-Al₂O₃-SiO₂-MgO melts. They introduced alumina particles to reduce the incubation time for crystallization. They also investigated the transition of crystal morphologies in different undercooled melts, i.e. from blocky to needle shaped and dendrites, as a function of temperature¹². However, the primary precipitated phase was not Wollastonite. In our previous work, the isothermal crystallization of CaSiO₃ in 42wt% CaO-10wt% Al₂O₃-48wt% SiO₂ melt at 1320°C and 1370°C was investigated by seeding the melt with Wollastonite particles through CSLM. That experimental technique has proven to be successful for characterizing isothermal

crystallization of minerals in silicate melts¹³. Nevertheless, the complicated effects of temperature and composition on the isothermal crystallization and growth of CaSiO_3 in CaO – Al_2O_3 – SiO_2 melts are still unclear.

In the present work, the crystallization behavior of Wollastonite (CaSiO_3) in different CaO – Al_2O_3 – SiO_2 melts was observed using CSLM over a wide range of temperatures and compositions. Several isothermal observations were made in a single experiment to avoid quenching effects. The effects of temperature and composition on the crystallization behavior of Wollastonite were analyzed based on thermodynamic and kinetic considerations. In the case of dendrite growth, the effect of temperature and composition on the growth rate and tip radius was investigated as well.

2. Experimental Procedure

2.1 Slag preparation

Different slag systems were selected in this work. Synthetic CaO – SiO_2 – Al_2O_3 slags were prepared by mixing the corresponding oxide powders with purity over 99.9%, and the detailed compositions are shown in Table I. Based on thermodynamic calculations, the slag compositions were chosen so that Wollastonite is expected to be the first precipitating phase during cooling. A Platinum crucible containing around 20g mixed oxide powders (of each composition in Table I) was placed in a bottom loading furnace (BLF, AGNI-ELT 160-02 Spring type) and heated up to 1630°C with a heating rate of 5°C/min in air and kept at this temperature for another 8 hours. Then the slags were poured onto a steel plate and quenched. Benefiting from the high cooling rate, all the obtained samples were amorphous.

2.2 Wollastonite seed preparation

Wollastonite particles were prepared to seed the crystallization in the experiments. Therefore, about 30g of CaO-SiO₂ powder mixture with molar ratio of 1 was put in a Platinum crucible. The samples were heated up to 1600°C in air at a rate of 5°C/min and hold at 1600°C for another two hours in the BLF, followed by a slow cooling down to 800°C at a rate of 0.5°C/min to avoid glass formation. The crystals were plate-like with a high aspect ratio. Afterwards, the sample was cooled down to room temperature at a rate of 5°C/min. The obtained slags were removed from the crucible and crushed into powders using a rotary mill. X-ray diffraction (XRD, Seifert, Ahrensburg, Germany) was used to identify the phase assemblage of the as milled powders (Fig. 1). The corresponding XRD pattern indicates that pure Wollastonite was obtained, since all the peaks could be well indexed as Triclinic Wollastonite.

2.3 CSLM observations

The set-up of the Confocal Scanning Laser Microscope (CSLM) has been described in detail in our previous work¹⁰. The temperature is controlled by a B-type thermocouple welded at the bottom of the sample holder. The HiTOS software in combination with a REX-P300 controller is used to program the temperature profiles. In order to ensure the accuracy of the measured temperatures, calibration has been performed using standard pure metal samples, e.g. copper, nickel and silver prior to the CSLM tests. A reproducible temperature difference of 40±5°C was observed between the thermocouple temperature and the sample temperature in the crucible. Hence, for example, if the set value for the PID controller of the CSLM was programmed at 1600°C, the actual sample temperature achieved in the crucible was only 1560°C. In this paper, all the marked temperatures are the corrected ones.

Before heating the sample, the CSLM chamber was flushed by argon for three times and then it was refilled with argon at a pressure of 1 atm. The Ar gas passed through a Restek triple filter for removing oxygen, moisture and hydrocarbons and a Restek high capacity oxygen scrubber before entering the CSLM chamber. The slag sample was first heated up to 1600°C for pre-melting and then quenched to room temperature in order to release all the gases absorbed by the powder and to realize a homogeneous distribution of glass in the crucible at the start of the in-situ experiments of isothermal CaSiO_3 crystallization.

After that, the Wollastonite seed was added at the top of the pre-melted slag in the crucible as a nucleus for crystallization. Then the slag sample with the Wollastonite particle on its surface was heated to the desired temperature. In earlier work¹³ we showed that the seeding nucleus (i.e. Wollastonite particles) can effectively avoid the formation of intermediate products in the nucleation process and accordingly allows a more direct observation and accurate analysis. After the temperature was increased to 1420 °C, it was controlled manually and different isothermal temperatures can be obtained. After observation at a fixed temperature for a certain period (1-5 minute), the sample was re-melted by heating up to 1420°C, then, it was quenched to another temperature for another observation. All the experiments were performed at a temperature higher than the second phase precipitation temperature (T2 in table I), which was calculated using FACTSage 6.3 (oxide database). This ensures that Wollastonite is the first precipitating phase during the solidification process. The CaSiO_3 crystallization process was recorded with a video recorder for further analysis. The crystal growth as a function of time, temperature, cooling rate and slag composition were obtained from the video images to obtain a better understanding of the crystallization thermodynamics and kinetics.

3. Results and discussion

The crystallization behavior of Wollastonite was studied based on the four different slag samples with initial compositions as shown in Table I. In the first three samples, the CaO to SiO₂ ratio was kept constant with a ratio of 0.875, while the content of Al₂O₃ was gradually increased. For sample D, the same Al₂O₃ content as for sample A was taken, but the CaO to SiO₂ ratio was increased from 0.875 to 1.0. These compositions were chosen to investigate the effects of, respectively, basicity (CaO/SiO₂) and Al₂O₃ content on the crystallization behavior of Wollastonite. It was verified through calculations with FACTSage 6.3 that Wollastonite is the primary precipitating phase during slag solidification for the compositions A-D. The Wollastonite precipitation temperatures T1 are given in table I. Other phases, e.g., CaAl₂Si₂O₈ and Ca₂Al₂SiO₇, will appear below the secondary precipitation temperature (T2) (also given in Table I). In order to avoid precipitation of these unwanted phases, all the experiments have been performed at temperatures between T1 and T2.

3.1 Wollastonite crystallization behavior in different slag systems at different temperatures

Distinct morphologies of the Wollastonite precipitates were found during an in-situ CSLM observation. The morphology was found to be strongly dependent on the experimental temperature. Table II lists for the 4 different slag systems the precipitate morphologies observed at different temperatures. In all cases, the morphology of the Wollastonite crystal changes from faceted to dendritic with decreasing temperature. The dendritic structure is easy to recognize due to the formation of characteristic primary and secondary dendrite arms.

As a representative example, Fig. 2 shows the morphology of the Wollastonite precipitate as observed at different temperatures for sample B. At 1380°C, the CaSiO₃ precipitates are faceted with hexagonal symmetry (Fig. 2a), which is believed to be a result of the intrinsic crystal symmetries of the polymorph β -Wollastonite. The dendritic morphology

forms from around 1360°C (Fig. 2b). The primary arms of the dendrite developed freely in all directions, and the secondary arms grew preferentially at an angle of 60° to the primary trunk. The growth of the secondary arms ceased when they reached those of the neighboring dendrites. In this way, a widely-spaced structure could develop. With further decrease of the crystallization temperature, the dendrite structure becomes finer (Fig. 2b, c and d).

The influence of undercooling and composition on the crystallization behavior has been compared for the three different slag compositions and is shown in Fig.3. At a constant undercooling of 40°C, a dendritic morphology developed in slags A and B (Fig. 3a, b), while it was still flake-like in slag D (Fig. 3c). For a larger undercooling of 120°C, the morphology was dendritic for all the slags. The dendrite structure obtained in slag D however was much finer than those obtained in slags A and B (Fig.3d-f). Since a smaller tip radius requires less material transport over shorter distances, it results in a faster growth rate under diffusion-controlled conditions. Therefore, the different Wollastonite crystalline morphologies observed in the CSLM tests were correlated with the differences in the growth rate of the dendrites as discussed in section 3.2.

Our experimental results also show that for a constant basicity (CaO/SiO_2), the undercooling required for dendrite formation decreases with increasing Al_2O_3 content. Moreover, a higher basicity results in a larger undercooling required for dendrite formation as seen in this section (Table II).

3.2 Growth rate during Wollastonite crystallization

The growth rate of the Wollastonite during isothermal holding was evaluated through the images obtained from the in-situ CSLM observation as follows. First, the position of the dendrite tip (point B in Fig. 4a) was measured as the distance from a reference point (A in Fig. 4a). The slope of the dendrite tip position as a function of time is then taken as the growth

rate of the dendrite. As an example, Figure 4(b) gives the dendrite tip position as a function of crystallization time as measured for slag B at 1360°C. The slope of the growth line represents the growth rate. It can be seen that the dendrite shows a linear growth with constant growth rate. The growth rate of faceted CaSiO_3 was determined by the same method and exhibited a linear growth behavior as well.

The growth rates obtained for different crystallization temperatures and for the different slag compositions are plotted in Fig 5. The data points above the dot dash line showed dendritic growth, while those below the line faceted growth. Generally speaking, the velocity first increases until a maximum value and then decreases slowly with increasing crystallization temperature. The temperatures at which the maximum growth velocity is reached are respectively 1340, 1320, 1310 and 1290°C for slags A, B, C and D. For slags with a fixed basicity (slag compositions A, B and C), the Wollastonite crystallization velocity decreases with Al_2O_3 content for a given crystallization temperature. Slag D, with a higher C/S ratio than the other slags shows a special behavior. Its crystallization velocity reaches a maximum value at around 1290°C (where the undercooling is approximately 110°C). This maximum velocity is much larger than that of the other slags. However, with increasing temperature, the crystallization velocity decreases very rapidly and becomes lower than that of slag A for temperatures above 1330°C (i.e. an undercooling of less than 80°C). The above observed temperature and composition dependence of Wollastonite growth rate will be discussed below.

3.2.1 Effect of crystallization temperature

Although only limited data points are available for the faceted growth in Fig.5, the temperature effect on the velocity of crystal growth (v) is obvious, i.e. v decreases with increasing temperature. It is well known that for most silicates, interface-controlled growth

leads to a faceted morphology. In this case, v can be expressed as a function of the latent heat (ΔH_c), viscosity (η) of the melt, undercooling (ΔT) and liquidus temperature (T_L) as given by the following equation¹⁴

$$v \approx A \Delta H_c \Delta T / \eta T_L \quad \text{Eq. (1)}$$

As temperature increases, both of $\Delta T/T_L$ and η will decrease accordingly, thus it is difficult to predict the change of the faceted growth velocity. However, based on the present experimental results, the effect of undercooling on the velocity seems to be much larger than that of viscosity, since temperature dependence of v is in line with the undercooling rather than viscosity (Fig.5).

A dendritic morphology forms due to a growth instability occurring when the diffusion of solute atoms to the crystal/liquid interface becomes a rate-limiting step. According to Fick's first law, the diffusion flux is proportional with the concentration gradient and the diffusion coefficient. Furthermore, the diffusion coefficient is inversely proportional with the viscosity, as described by the Einstein-Stokes equation¹⁵

$$D = \frac{k_B T}{6\pi r \eta} \quad \text{Eq. (2)}$$

where k_B is the Boltzmann's constant, T refers to the absolute temperature, r is the radius of the spherical particle and η is the viscosity. Figure 6 gives the relation of slag viscosity and temperature, in which the slag viscosity was calculated with the Urbain model¹⁶. In general, slag viscosity increases with decreasing temperature, indicating that the dendrite growth rate should increase with temperature. Our observations (Fig 5) showed that this temperature dependence occurs in a certain temperature range. At higher temperatures, however, the dendrite growth velocity appeared to decrease with temperature (see Fig 5, e.g. between 1320-

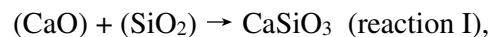
1340°C for slag B). This indicates that at higher temperature (namely, those just below the temperature region where faceted growth becomes more favorable) the thermodynamic driving force, in terms of undercooling, plays a dominant role in determining the dendrite growth rate.

3.2.2 Effect of slag composition

Apart from the temperature, the velocity of the CaSiO_3 dendrite growth strongly relies on the slag composition. Figure 5 shows that in the higher temperature regions, where the growth rate of Wollastonite dendrite increases with decreasing temperature, the growth rate of Wollastonite crystallization decreases with undercooling at a certain temperature (see Table 1 for the T1 temperatures for the different slag compositions). Hence, the predominant factor here is the thermodynamic driving force, which directly supports the discussion in section 3.2.1. At lower temperatures, the growth rate is highest in slag D, and it decreases as a function of slag composition as slag D > slag A > slag B > slag C. This composition-velocity relation indicates the crystallization process limited by mass diffusion. Considering the reverse relationship between viscosity and the diffusion coefficient (Eq.2), such trend could be interpreted primarily by the slag viscosity (See Fig.6). For a fixed basicity, i.e. for slags A to C, the viscosity increases with increasing alumina content. Benefiting from the higher basicity in slag D, it has a substantially lower viscosity compared to the other slags. As a result, the highest growth velocity could be reached for this composition.

The composition-velocity relationship of CaSiO_3 dendrite growth at lower temperatures can be explained by the diffusion behavior of Ca^{2+} as well. Since the molar ratio between CaO and Al_2O_3 is much larger than 1 for all considered slags, $[\text{AlO}_4]^-$ tetrahedron is balanced with 0.5Ca^{2+} in these cases, while the residual Ca^{2+} ions can diffuse to form Wollastonite. Therefore, Ca^{2+} can be considered as a network modifying cation while the Si^{4+} and Al^{3+}

serve as network formers, according to previous studies^{17, 18}. Since the precipitation of Wollastonite occurs by reaction I,



both Si^{4+} and Ca^{2+} ions could be considered as the diffusing species.

However, Si^{4+} , as the network former, can hardly diffuse. In view of this, the high relative mobility of the network modifying cation Ca^{2+} determines the crystallization velocity. The higher Al_2O_3 amount will increase the slag viscosity¹⁹, therefore decreasing the diffusibility of Ca^{2+} in the slag, which will result in a lower crystallization velocity. For slags A, B and C, the content of Al_2O_3 changes as follows $\text{C} > \text{B} > \text{A}$ and accordingly the crystallization velocity sequence is expected to largest for slag A and lowest for slag C, as is indeed seen experimentally (see Fig.5).

3.3. Calculation of the dendrite tip radius from the measured dendrite tip velocities

Our previous study¹³ shows that the current small-scale experimental set-up can ensure an isothermal condition, which can effectively avoid the occurrence of convection inside. Thus, Ivantsovs theory²⁰ can be employed to calculate the dendrite tip radius. According to Ivantsovs theory, the dendrite tip radius at steady state growth is related to the growth rate and the Peclet number P as

$$P = \frac{\rho v}{2D} \text{ Eq. (3)}$$

where ρ is dendrite tip radius, v is dendrite tip velocity and D is the diffusion coefficient in the melt. It is assumed in this work that the dendrite shape is as assumed in Ivantsovs theory. Then the Peclet number and the supersaturation Δ can be related using Ivantsovs formula, giving

$$\Delta = \frac{xL - x0}{xL - xS} = \sqrt{\pi P} \exp(P) \operatorname{erfc}(\sqrt{P}) \quad \text{Eq. (4)}$$

$$\text{with } \operatorname{erfc}(x) = \frac{2}{\sqrt{\pi}} \int_x^\infty e^{-t^2} dt \quad \text{Eq. (5)}$$

in 2D, and as

$$\Delta = \frac{xL - x0}{xL - xS} = P \exp(P) Ei(P) \quad \text{Eq. (6)}$$

$$\text{with } Ei(P) = \int_{-\infty}^P \frac{e^t}{t} dt \quad \text{Eq. (7)}$$

in 3D, where, xL and xS respectively indicate the equilibrium content of the diffusion component (for solidification or crystallization) in melt and solid crystal at the interface. $x0$ is the initial content of the diffusion component in the melt. In our previous study¹³, we also showed that, since the solidification occurs at the surface of the melt, the growth behavior in the CSLM can vary between the 2D and 3D mode of Ivantsovs theory, depending on how much the dendrite tip is submerged in the melt. Since the position of the dendrite tip with respect to the melt surface depends on the surface tensions of the solid and liquid and the solid-liquid interfacial energy, it can vary with temperature and composition. Therefore, also in this work, our experimental data were compared with the Ivantsovs relations for 2D and 3D growth behavior.

Considering CaO as the rate limiting diffusing component in Wollastonite crystallization, the Peclet number can be calculated solving Eqs. (5) and (7) for the 2D and 3D case, respectively, using Maple software. Substituting the calculated Peclet number P , the diffusion coefficient of CaO in the slag at different temperatures and the dendrite growth rate as measured from the CSLM experiments at different temperatures into Eq. 3, the dendrite tip

radii could be calculated. Figs.7 (a) and (b) show the calculated tip radii of the Wollastonite dendrites assuming 2D and 3D behavior, respectively. The calculated 2D dendrite tip radii are in the range of 0.03 to 0.52 μm (Fig.7a). Moreover, except for slag D, the tip radius decreases with increasing Al_2O_3 content and temperature, while the experimentally observed micrographs shown in Fig.3, show a finer dendritic structure with decreasing temperature and Al_2O_3 content. As discussed in section 3.2, increasing the Al_2O_3 content hinders the diffusion of Ca^{2+} to the liquid/solid interface, which consequently lowers the crystallization velocity and results in a coarser dendrite structure. Therefore, for the considered temperature and composition range, the 2D mode of Ivantsov's theory appears to be unsuitable to describe the temperature dependence of dendrite growth behavior observed in the CSLM experiments. The 3D model gives a dendrite tip radius between 0.77 to 8.82 μm (Fig. 7b) and its temperature dependence is in good agreement with the experimentally observed dependence as shown in Fig.3. At a given isothermal temperature, the value of dendrite tip radius is in a sequence of $C > B > A$, indicating that a finer dendrite structure is formed at a lower Al_2O_3 concentration. Therefore, qualitatively, the 3D variant of Ivantsov's theory describes well the overall growth behavior observed in the CSLM experiments.

Several dendrite radii could be measured the images from CSLM, as described in Fig.8. Comparison of the calculated radii for the 2D and 3D mode with the measured dendrite radii (ρ_{exp}) as shown in Fig. 9 (also see the data in Table III), shows that the dendrite growth observed in all slags is between the predictions for the 2D and 3D growth mode. At low temperature, the growth conditions in the CSLM appear to be close to 2D, whereas at higher temperatures the conditions shift more towards 3D growth behavior, i.e. with increasing temperature the dendrite tip is submerged further into the melt. This is probably caused by the decrease of slag density with increasing temperature. Similar phenomena were also reported in Zhou's work²¹.

4. Conclusions

The crystallization of Wollastonite in $\text{CaO-Al}_2\text{O}_3\text{-SiO}_2$ melts was observed in-situ using a Confocal Scanning Laser Microscope. The different slag systems were selected based on thermodynamic calculations. The observations were taken for compositions and temperatures for which Wollastonite is the primary precipitating phase and the following observations were made:

- (1) At high temperatures, a hexagonal planar growth is observed in all four slags and at lower temperatures the morphology changes into dendritic. The undercooling required for dendrite formation decreases with increasing Al_2O_3 content for the same slag basicity (CaO/SiO_2) and increases with increasing basicity. The dendritic structure is finer for higher crystallization velocities.
- (2) For a given temperature, a constant growth rate was found for both faceted and dendritic growth in all slags. For dendritic growth, when temperature decreases, the growth rate first increases and then decreases. Furthermore, it decreases with increasing Al_2O_3 content for equal basicity (CaO/SiO_2), since the Al_2O_3 increases the slag viscosity, therefore hindering the diffusion of Ca^{2+} to the liquid/solid interface, which consequently lowers the crystallization velocity.
- (3) By comparing the measured dendrite tip radii with the calculated tip radii using Ivantsov's 2D and 3D model, it is clear that the experimental dendrite growth conditions in the presented CSLM experiments were between 2D and 3D diffusion controlled growth. With increasing temperature, it changes from closer to 2D behavior, i.e. the dendrite tip is located at the melt surface, to closer to 3D, i.e. the dendrite tip position is below the surface of the melt, this is probably caused by the decrease of slag density with increasing temperature.

Acknowledgements

The author Jingjing Liu thanks for the financial support from China Scholarship Council (CSC).

References

- [1] Z.T. Zhang, J. Liu and P. Liu. Crystallization Behavior in Fluoride-Free Mold Fluxes Containing $\text{TiO}_2/\text{ZrO}_2$. *Journal of Iron and Steel research international* 18(2011) 31–37.
- [2] G.H. Wen, X.B. Zhu, P. Tang and X. Yu. Influence of Raw Material Type on Heat Transfer and Structure of Mould Slag. *ISIJ International* 51(2011) 1028–32.
- [3] M. Valdez, G. S. Shannon, and S. Sridhar, The Ability of Slags to Absorb Solid Oxide Inclusions. *ISIJ International* 46(2006) 450–457.
- [4] Mc Millan PW. *Glass-ceramics*. Academic Press; 1979.
- [5] Cao JW and Wang Z. Effect of Na_2O and heat-treatment on crystallization of glass-ceramics from phosphorus slag. *Journal of Alloy and Compounds* 557(2013) 190-195.
- [6] H. G. Ryu, Z. T. Zhang, J. W. Cho, et al., Crystallization Behaviors of Slags through a Heat Flux Simulator. *ISIJ International* 50(2010) 1142-1150.
- [7] Y. Kashiwaya, T. Nakauchi, K. S. Pham, et al., Crystallization Behaviors Concerned with TTT and CCT Diagrams of Blast Furnace Slag Using Hot Thermocouple Technique. *ISIJ International*, 47(2007) 44-52.
- [8] Jones P, Desmet D, Guo M, Durinck D, Verhaeghe F, Van Dyck J. Using confocal scanning laser microscopy for the in situ study of high-temperature behaviour of complex ceramic materials. *Journal of the European Ceramic Society* 27(2007) 3497–507.

- [9] Z. T. Zhang, G. H. Wen, J. L. Liao, et al., Observations of Crystallization in Mold Slags with Varying $\text{Al}_2\text{O}_3/\text{SiO}_2$ Ratio. *Steel Research International* 81(2010) 516-528.
- [10] Liu, J, Guo, M Jones, PT, Verhaeghe F, Blanpain, B and Wollants, P. In situ observation of the direct and indirect dissolution of MgO particles in $\text{CaO-Al}_2\text{O}_3\text{-SiO}_2$ -based slags. *Journal of the European Ceramic Society* 27(2007) 1961-72.
- [11] H.B. Yin, H. Shibata, T. Emi, et al., In Situ Observation of Collision Agglomeration and Cluster Formation of Alumina Inclusion Particles on Steel Melts. *ISIJ International* 37(1997) 936–45.
- [12] Orrling C, Sridhar S, Cramb AW. In situ observation of the role of alumina particles on the crystallization behavior of slags. *ISIJ International* 40(2000) 877–85.
- [13] J. Heulens, B. Blanpain, N. Moelans. Analysis of the isothermal crystallization of CaSiO_3 in a $\text{CaO-Al}_2\text{O}_3\text{-SiO}_2$ melt through in situ observations. *Journal of the European Ceramic Society* 31(2011) 1873–1879.
- [14] R. James Kirkpatrick, Crystal growth from the melt: A review. *American Mineralogist*, 60(1975) 798-814.
- [15] J. T. Edward, Molecular volumes and the Stokes-Einstein Equation. *Journal of Chemical Education* 47(1970) 4.
- [16] G. Urbain, Viscosity estimation of slags. *Steel research* 58(1987) 111-116.
- [17] M. L. F. Nascimento, E. B. Ferreira, and E. D. Zanotto, Kinetics and mechanisms of crystal growth and diffusion in a glass-forming liquid. *Journal of Chemical Physics* 121(2004) 18.

- [18] R. G. Duan, K. M. Liang, and S. R. Gu, A study on the mechanism of crystal growth in the process of crystallization of glasses. *Materials Research Bulletin* 33(1998) 1143–1149.
- [19] X.L. Tang, Z.T. Zhang, M. Guo, M. Zhang and X. D. Wang, Viscosities Behavior of CaO-SiO₂-MgO-Al₂O₃ Slag With Low Mass Ratio of CaO to SiO₂, and Wide Range of Al₂O₃ Content. *J. Iron Steel Res Int.* 18 (2010) 01-06.
- [20] Ivantsov G. *Dokl Akad Naut SSR* 58(1947) 567.
- [21] L.J. Zhou, W. L. Wang, and F. J. Ma, A kinetic study of the effect of basicity on the mold fluxes crystallization. *Metallurgical and materials transactions B* 43B(2012) 354-362.

Table and Figure captions:

Table I Slag compositions and transition temperatures of the considered slag samples

Table II. The precipitated crystal morphologies obtained at different temperatures for the four different slag compositions.

Table III. Dendritic tip radius calculated from Ivantsov theory in 2D and 3D compared with experimentally measured tip radii.

Fig.1 XRD pattern of synthetic CaO-SiO₂ powder prepared as described in section 2.2

Fig.2 Growth morphologies observed for Slag B at different temperatures.

Fig.3 Growth morphologies observed for different slag compositions (the samples A, B and D with compositions as given in Table I) at different undercoolings (40 and 120°C).

Fig.4(a) Micrograph of crystallizing Wollastonite at 1360°C in slag B; (b) Dendrite tip position as a function of time for slag A at 1330°C. The dendrite tip growth rate is determined as the slope of the growth line, giving 7.24µm/s

Fig.5 Measured growth rate as a function of temperature in different slags. The data points above the dotted line showed dendritic growth and those below the dotted line faceted growth

Fig.6 Viscosity as a function of undercooling for the slags A, B, C and D, calculated using the Urbain model ¹⁶

Fig.7 Calculated dendrite tip radius as in 2D and 3D as a function of temperature. (a) 2D, (b) 3D.

Fig.8 The drawing showing the determination of dendrite tip radius from a CLSM image.

Fig.9 Calculated and experimental dendrite tip radius as in 2D and 3D as a function of temperature. (a) slag A, (b) slag B.